COMMUNICATION

PCCP
www.rsc.org/pccp

Investigating the structure of boron nitride nanotubes by near-edge X-ray absorption fine structure (NEXAFS) spectroscopy†

Tirandai Hemraj-Benny,[a] Sarbajit Banerjee,‡[a] Sharadha Sambasivan,[b] Daniel A. Fischer,[b] Weiqiang Han,[c] James A. Misewich[d] and Stanislaus S. Wong*[ad]

[a] *Department of Chemistry, State University of New York at Stony Brook, Stony Brook, NY 11794-3400. E-mail: sswong@notes.cc.sunysb.edu; sswong@bnl.gov*
[b] *Materials Science and Engineering Laboratory, National Institute of Standards and Technology, Gaithersburg, MD 20899*
[c] *Center for Functional Nanomaterials, Brookhaven National Laboratory, Upton, NY 11973*
[d] *Materials Sciences Department, Brookhaven National Laboratory, Bldg. 480, Upton, NY 11973*

Received 5th October 2004, Accepted 9th February 2005
First published as an Advance Article on the web 17th February 2005

Herein, we demonstrate that NEXAFS is a very effective technique at (a) identifying the phases of boron nitride nanotubes with the potential of distinguishing between hexagonal BN and cubic BN, and (b) monitoring the presence of defects and degree of crystallinity in nanoscale samples. Specifically, a prepared sample of boron nitride nanotubes was characterized by NEXAFS. Our results show that the sample consisted of hexagonal BN tubes that were highly crystalline and sp^2-hybridized.

Introduction

Nanomaterials are widely studied because of their potential applications in fields as diverse as electronics, nanocatalysis, and field emission. Though carbon nanotubes have been extensively analyzed in this context, nanostructures, made of other materials that commonly exist in graphite-like layered forms, such as boron nitride nanotubes, can also be fabricated with a higher degree of control over diameter and helicity.

Unlike carbon nanotubes, the band gap for boron nitride does not depend as sensitively on diameter and helicity but is rather constant at 5.5 eV.[1,2] In addition, boron nitride possesses tremendous thermal stability and strength, which make them ideal for applications requiring high-strength, lightweight materials.[3,4] The Young's modulus of multiwalled BN nanotubes, for instance, is 1.22 ± 0.4 TPa.[5] Because of their slightly more ionic nature as compared with carbon nanotubes,[3] BN tubes are expected to flex more easily than carbon nanotubes, though still retaining a high degree of stiffness.[3,6]

Other applications for these materials would be as high temperature transistors, photoluminiscent devices, high temperature lubricants, microwave and infrared transparent materials,[7] and as 'superstrong' supports in polymer matrices and composite materials.[8,9] BN and mixed BCN systems already demonstrate promise as stable field emitters for use in flat panel displays.[10,11] Moreover, these systems have been shown to have excellent gas storage capacities with potential for use in fuel cells.[12,13] Collapsed BN nanotubes were found to store up to 4.2% by weight of hydrogen. With multiwalled BN nanotubes, the value was ~1.8–2.6% by weight of hydrogen.

Boron nitride can exist in metastable rhombohedral (r-BN), zinc-blende cubic (c-BN) or wurtzite (w-BN) phases, though its most stable phase is hexagonal (h-BN).[14,15] From a structural point of view, c-BN is analogous to diamond, whereas h-BN is similar to that of graphite. It is noteworthy that whereas h-BN and r-BN demonstrate sp^2 hybridization, c-BN and w-BN exhibit sp^3 hybridization.

Some common techniques used in distinguishing c-BN from h-BN, and hence, sp^3 from sp^2 hybridization, include X-ray diffraction (XRD), Raman spectroscopy, infrared spectroscopy (IR), electron energy loss spectroscopy (EELS), and near-edge X-ray absorption fine structure spectroscopy (NEXAFS). However, vibrational spectroscopies and XRD are generally found not to be suitable for studying the structure of nanocrystalline samples due to phonon confinement and Scherrer broadening effects, respectively. Conversely, near-edge X-ray absorption spectroscopy has the advantage of being a nondestructive analytical tool and is inherently more sensitive to the bonding configurations of the different types of atoms, as well as to the geometry of the structure, making it a more localized technique. Thus, whereas there is significant broadening of Raman peaks as the crystalline domain size decreases in nanocrystalline samples, element-specific NEXAFS spectra are not similarly degraded.[16]

More specifically, NEXAFS spectroscopy involves the excitation of electrons from a core level to partially filled and/or unoccupied states in the conduction band. Hence, the peak positions and spectral line shapes in a NEXAFS spectrum are directly related to the nature of these unoccupied electronic states. The fact that the dipole-like electronic transitions probed occur from core states, which have well-defined orbital-angular momenta, into empty electronic (*e.g.* antibonding) states accounts for the relative sensitivity of NEXAFS to local chemical bond order. Hence, from the symmetry of the final state, it is thus possible to distinguish between sp^2 and sp^3 bonding, since they are π-like and σ-like, respectively.[17,18]

Because this technique is not particularly sensitive to domain size, NEXAFS has been previously used to characterize bonding in and to differentiate among different BN phases in a wide range of samples, including microcrystals,[19] fine-grained or amorphous films,[14] and randomly oriented powders.[20] Nitrogen interstitials, boron clustering, as well as the presence of defects have also been observed in bulk and thin films of boron nitride[21] while bonding modifications (resulting in sp^3-bonding formation) and defect content induced by ion implantation

† Electronic supplementary information (ESI) available: Fitted boron K-edge and carbon K-edge spectra of BN nanotubes and bulk BN. See http://www.rsc.org/suppdata/cp/b4/b415423a/

‡ Current address: Department of Applied Physics and Applied Mathematics, Columbia University, New York, NY 10027.

DOI: 10.1039/b415423a

have been studied by the same group using NEXAFS.[15] All of this analysis was performed with minimal sample destructiveness and with a greater energy resolution as opposed to conventional EELS. NEXAFS has recently been used to prove that the conduction band of h-BN/Ni(111) system is different from that of the bulk.[22] In addition, NEXAFS confirmed that nanocrystalline cubic BN films containing a significant fraction of sp^3 bonds can be synthesized using a low-density, supersonic arcjet flow.[23]

We have previously reported on the use of NEXAFS as a valuable tool in probing the surface chemistry, alignment, and electronic structure of carbon nanotubes.[24,25] Herein, we demonstrate that NEXAFS is a very effective technique at (a) identifying the phases of boron nitride nanotubes with the potential of distinguishing between hexagonal BN and cubic BN, and (b) monitoring the presence of defects and degree of crystallinity in nanoscale samples. Specifically, a prepared sample of boron nitride nanotubes was characterized by NEXAFS. Our results confirm that the sample consisted of h-BN tubes, that were highly crystalline and sp^2-hybridized.

Experimental

Boron nitride samples

Bulk cubic and hexagonal boron nitride samples were obtained from Reade Advanced Materials and Sigma-Aldrich, respectively. Boron oxide standard samples were purchased from Sigma-Aldrich.

Established methodologies for creating nanoscale BCN and BN structures can be classified as (i) arc discharge, (ii) laser ablation, and (iii) pyrolysis of organic precursors over metal catalysts.[26] In the current experiment, the tubes used were prepared by a substitution reaction, meaning that the carbon atoms in the carbon nanotubes were substituted by other atoms to form the required boron nitride nanotubes.[27–29] Specifically, boron oxide gas, generated from B_2O_3 powder, was reacted with relatively pure-shell multi-walled carbon nanotubes (diameters of $\sim$10 nm) in a flowing nitrogen atmosphere at 1773 K to produce BN nanotubes within a grey wool-like product. By TEM,[27–29] the nanotubes had a diameter range of a few nm and lengths of up to a few micrometres with an interplanar spacing of $\sim$0.335 nm.

As such, the resulting BN nanostructures were predominantly multi-walled nanotubes though a large number of double-walled nanotubes were also observed. Extensive structural characterization of these nanostructures has been previously reported.[27–29] X-ray diffraction (XRD) data indicated that the BN nanotubes consisted of almost equal amounts of h-BN and r-BN and it was clear that the degree of crystallization was better than that of the starting CNTs. In addition, electron energy loss spectroscopy (EELS) data suggested that the nanotubes in the product consisted of essentially completely BN nanotubes without any noticeable trace of carbon. Data from the electronic supplementary information (ESI)† confirms this assertion. The low edge jump intensity from the C K-edge spectra suggests a very insignificant amount of carbon in the samples. Furthermore, the C *K*-edge shows a relatively strong σ^* peak characteristic of sp^3-hybridized carbon that is likely to possess an amorphous origin as opposed to being derived from sp^2-hybridized nanotubes. Indeed, the high purity of BN nanotubes available through this carbon nanotube substitution reaction, particularly the absence of extensive amorphous or non-tubular BN in the samples, suggested that this nanostructured sample was ideal for reliable and interpretable measurements using NEXAFS spectroscopy.

NEXAFS measurements

B *K*-edge and N *K*-edge NEXAFS spectra were taken using the U7A NIST/DOW end station at the National Synchrotron Light Source (NSLS) at Brookhaven National Laboratory. The partial electron yield (PEY) signal was collected using a channeltron electron multiplier with an adjustable entrance grid bias (EGB). A negative bias of 50 V was applied to reject extraneous background due to low energy electrons. Data were recorded in a UHV chamber with an incident X-ray resolution of 0.1 eV. In addition, the spectra were collected at room temperature with the incident beam at the magic angle of 54.7°, relative to the surface, to remove any polarization dependence of the pi-type states on the X-ray source. For the actual data collection, the samples were contained within a stainless steel washer, which was then pressed onto a Cu tape and mounted onto a sample bar inside a vacuum chamber. To eliminate the effect of incident beam intensity fluctuations and monochromator absorption features, PEY signals were normalized using the incident beam intensity obtained from the photoemission yield of a clean Au grid. In order to prevent charging of the insulating BN, charge compensation with low energy electrons was used.

The edge jump for the B K-edge is defined as the intensity difference at energies before the onset of B K-edge measurements (*e.g.* $<$190 eV) and after the transitions (*e.g.* $>$217 eV). These spectra have been processed through pre- and post-edge normalization routines after energy calibration of the Au grid located upstream of the sample. Specifically, the post edge-jump normalization was performed by dividing the pre-edge-jump normalized spectra by the edge jump intensity obtained far above the K-edge, beyond 217 eV. Thus, changes in spectral intensity observed arise from chemical changes in the system and are independent of total boron content. In addition, bulk h-BN and BN nanotube spectra have been fitted in the energy range of 188–220 eV, with Gaussians and an arctangent to fit the resonances and the edge jump, respectively, as seen in the ESI.† Analogous pre- and post-edge normalization of the N K-edge spectra were also performed at values $<$396 eV and beyond 430 eV, respectively. To account for the presence of carbon, pre-edge normalization of C K-edge spectra was accomplished at values $<$280 eV.

Results and discussion

Fig. 1 shows a comparison of B K-edge spectra of (a) bulk c-BN, (b) bulk h-BN, (c) BN nanotubes, and (d) boron oxide standards obtained at the magic angle ($\theta = 54.7°$). Comparing the B 1s K-edge spectra of bulk h-BN and of BN nanotubes, a

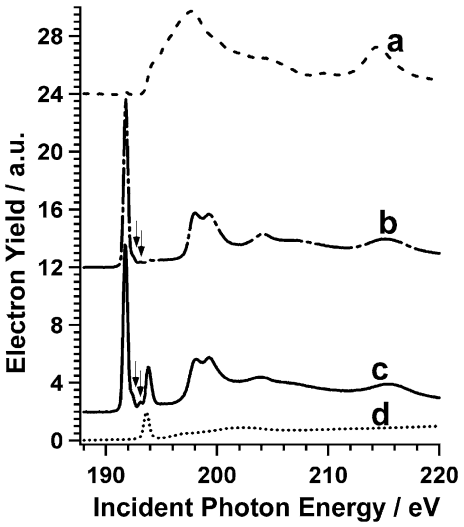

Fig. 1 Boron K-edge spectra, taken at retarding potential of −50 V and at the magic angle ($\theta = 54.7°$). (a) (--): bulk c-BN sample; (b) (-·-): bulk h-BN sample; (c) (—): boron nitride nanotube (BN-NT) samples; and (d) (···): boron oxide sample. All spectra have been pre- and post-edge normalized, as described in the experimental section.

number of similarities can be observed, which strongly suggests that they are structurally-related materials with the same chemical composition. The prominent, narrow and intense peak at 191.8 eV corresponds to the B 1s $\rightarrow$ π^* resonance, which is associated with sp^2 hybridization and planar bonding.[14,18] Two nearby resonances at around 198.5 and 199.7 eV correspond to the excitation to a single energy-split σ^* state.[30] However, the feature appearing at 203.6 eV can be attributed to the nitrogen K-edge, due to the presence of a second harmonic in the monochromatic X-ray beam.[19] We further confirmed this assertion by increasing the bias (EGB) beyond –170 eV, which eliminated features from the B K-edge; the residual spectra[31] indeed reflected signals emanating from the second harmonic contribution of nitrogen.

The broad peak at 215.3 eV can be assigned to a σ^* resonance.[23] Theoretically, the peaks observed between 197 and 216 eV have been analyzed by means of overlap population diagrams.[32] Specifically, it was predicted that peaks at 198.3 eV and 199.6 eV originate from antibonding interactions involving N-2s and B-$2p_{xy}$ orbitals, while the broad peak at 203.6 eV possibly originates from antibonding interactions involving N-$2p_{xy}$ and B-$2p_{xy}$ orbitals as well as a contribution from the second harmonic N-peak. In addition, the B–2s orbital contributes to the peak at 198.3 eV.

Although the B K-edge NEXAFS spectrum of the BN-NTs is very similar to that of the bulk h-BN, there were some differences noted. For example, an additional peak at 193.8 eV was noted in the BN nanotube spectrum, Fig. 1 and SI. Comparison with the spectrum[31] of the boron oxide standards, taken at U7A, confirms that this extraneous peak originates from the presence of boron oxide in the BN nanotube sample. The fact that boron oxide was indeed associated with the preparation of these BN nanotubes strongly suggests that the additional peak originated from unreacted boron oxide.

For the bulk c-BN sample, there were no detectable π^* features present in the B K-edge due to the predominant sp^3 hybridization. The spectrum was dominated by an absorption edge, appearing approximately at 194.2 eV, which corresponds to transitions from the 1s level to the σ^* continuum states in the conduction band.[18] In addition, the nitrogen second harmonic was also observed in the c-BN spectrum, around 203 eV, and the peak at 214.3 eV is believed to arise from a σ^* resonance.

From the data obtained, as seen in Fig. 1, it can be concluded that the sample of BN nanotubes studied indeed consists of tubes with hexagonal type bonding (h-BN). Hence, the hybridization is likely sp^2 and it is further expected that the BN nanotubes exist as graphitic-like layer forms, consistent with the other characterization data.[27] Moreover, since the dominant feature at 197.7 eV observed in the c-BN spectrum was not noted in the BN nanotube spectrum, it can be reasonably assumed that there were likely no cubic phases present within these nanotubes. The similarity between BN nanotubes and h-BN has been previously noted in EELS spectroscopy.[33]

In addition, it should be noted that the B K-edge spectra of both bulk h-BN and BN-NTs samples consist of two additional features, specifically at 192.4 eV and 193 eV with varying intensities, indicated by the arrows (Fig. 1 and SI). These specific peaks may likely originate from defects in the hexagonal bonding, specifically from boron atoms bound to two nitrogens and boron atoms bound to a single nitrogen.[15] While it has been argued that these types of features may arise from interactions between the BN monolayer and the underlying substrate (such as Ni (111)) upon which the BN is epitaxially grown,[22] the samples analyzed herein were clearly freestanding bulk and nanotube samples. Hence, these samples could not have had any appreciable interactions with a substrate to account for the presence of the observed peaks in question.

Thus, assuming the defect hypothesis is correct, because the peaks in the bulk h-BN sample possess a lesser intensity as compared with the BN nanotube sample, then there were likely to have been fewer defects in the bulk sample as opposed to the BN nanotube sample. The increased intensity of these peaks in the BN nanotube sample may arise from initial defects found on the carbon nanotube templates that were used in the synthesis of BN nanotubes.[27–29] Moreover, this could be a diagnostic of the curvature-induced rehybridization of bonds within the nanotube structure. However, it is evident that the peaks associated with our BN nanotubes, which appear as relatively small, shoulder-like features, are neither as well defined nor as prominent as compared with the corresponding literature spectra for ion-irradiated thin films.[15] Therefore, it can be assumed that our sample of BN nanotubes is highly crystalline. This conclusion corroborates previous TEM and XRD data that the BN nanotubes were of a more highly crystalline nature than the starting carbon nanotubes.[27]

Fig. 2 shows the N K-edge spectra of c-BN, h-BN, and BN nanotubes, respectively. The peaks at 403.4 eV and 402.9 eV of the h-BN and BN nanotube samples, respectively correspond to π^* resonance transitions. Other peaks at the higher energies, specifically at 410.0 eV and 417.4 eV for the h-BN and 409.9 eV and 417.5 eV for the BN nanotube samples, could be ascribed to σ^* resonances. By contrast, the primarily sp^3-bonded c-BN sample did not show any π^* features; rather, overlapping features observed corresponded to σ^* resonances.

In general, in comparing the N K-edge spectra obtained for the bulk h-BN and the BN nanotube samples, the spectra consisted of essentially similar features. We also observe that there were no additional peaks seen in the BN nanotube spectra as compared with that of the h-BN sample, which would have been a clear diagnostic for the presence of defects, such as B vacancies or tetrahedral nitrogen on the tubes. These results further confirm that the BN nanotube sample studied likely consists of highly crystalline, hexagonally-bonded tubes.

It should be noted that there was an observed negative shift of 0.5 eV (to lower energy) of the π^* resonance of the BN nanotube sample as compared with that of the bulk h-BN. Nonetheless, there were no significant variations in the FWHMs or in the intensities of these peaks. Similarly, there was also a negative σ^* resonance shift of 0.1 eV in the spectrum of the BN nanotubes as compared with that of the h-BN spectrum. The latter σ^* shift may result from a minor increase in B–N bond lengths,[18] but due to its small magnitude, is more likely a result of issues related to experimental precision.

While it has been reported that there is a mixture of h-BN and r-BN present in the particular sample of BN nanotubes studied herein, it should be noted that the presence of this mixture alone probably cannot account for the observed shift in the π^* resonance. It has been previously demonstrated[14] that using NEXAFS spectroscopy alone, it is very difficult to distinguish between rhombohedral and hexagonal phases of BN, because of the nearly identical local bonding and chemical

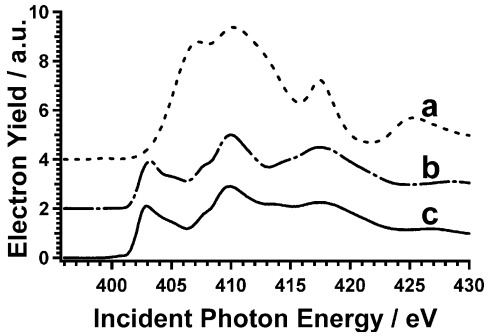

Fig. 2 Nitrogen K-edge spectra, taken at retarding potential of −50 V and at the magic angle ($\theta = 54.7°$). (a) (--): bulk c-BN sample; (b) (---): bulk h-BN sample; and (c) (—): boron nitride nanotube (BN-NT) samples. All spectra have been pre- and post-edge normalized as described in the experimental section.

environment for both phases. That is, both phases have a similar sp^2, conjugated π-bond structure, associated with their dominant $1s \rightarrow \pi^*$ resonances. These phases essentially differ only in their interplanar interactions, which is notably weaker than the intraplanar bonding/electronic interactions that primarily affect NEXAFS spectra local structure.

A possible explanation as to why the observed shift is more pronounced in the N K-edge as opposed to the B K-edge of the BN nanotubes is related to the fact that in these tubular motifs, the nitrogen atom is more structurally affected. Boron atoms tend to retain their sp^2 bonding with bond angles of 120°, whereas nitrogen atoms evolve to an admixture status, involving sp^3 hybridization, thereby leading to smaller bond angles.[34] In addition, as N is the more electron rich species in the polar B–N bond, it likely contributes most of the bonding electron density. Thus, it is not surprising that the N K-edge would be more sensitive to the curvature/non-planarity effect and the resulting destabilization of the bond in the tube. Hence, because the energy dispersion of the π* band of the BN nanotubes is different from that of h-BN due to the curvature of BN honeycomb layers,[35] morphology is likely a contributing factor to the observed shift.

In analogous carbon nitride systems, negative shifts in the π* resonances to lower energy have been attributed to the lack of participation of the lone pair of electrons associated with the nitrogen in the overall π-aromatic system.[36] Charge transfer from the N to the B atoms induced by the higher electronegativity of N might potentially be considered as an alternative explanation for the energy displacements.[37] Future work will necessitate detailed theoretical investigations, including DOS calculations, to fully investigate the precise relationship of structure with respect to the spectra obtained.

Conclusions

In conclusion, NEXAFS is an effective tool at providing valuable structural information about boron nitride nanotubes. It was determined that for the sample of BN nanotubes studied, h-BN was indeed present in graphite-like form. In addition, these nanotubes were found to be highly crystalline and have a low defect density. Thus, we note that our results further confirm that the substitution reaction reported previously[27] is an effective method at producing high quality BN nanotubes.

Acknowledgements

The authors would like to thank Dr Zugen Fu for collection of the B_2O_3 calibration NEXAFS spectrum taken at the U7A NIST/DOW beamline, located at the National Synchrotron Light Source (NSLS) at Brookhaven National Laboratory (BNL). We acknowledge support of this work through startup funds provided by the State University of New York at Stony Brook as well as BNL. Acknowledgment is also made to the National Science Foundation (DMII-0403859 and CAREER award DMR-0348239) and to the donors of the Petroleum Research Fund, administered by the American Chemical Society, for support of this research. SSW thanks 3M for a non-tenured faculty award. Research was carried out in part at the NSLS at BNL, which is supported by the US Department of Energy under contract number DE-AC02-98CH10886.

References

1 A. Rubio, J. L. Corkill and M. L. Cohen, *Phys. Rev. B*, 1994, **49**, 5081.
2 X. Blase, A. Rubio, S. G. Louie and M. L. Cohen, *Europhys. Lett.*, 1994, **28**, 335.
3 E. Hernandez, C. Goze, P. Bernier and A. Rubio, *Phys. Rev. Lett.*, 1998, **80**, 4502.
4 L. A. Chernozatonskii, E. G. Gapern, I. V. Stankevich and Y. K. Shimkus, *Carbon*, 1999, **37**, 117.
5 N. G. Chopra and A. Zettl, *Solid. State. Commun.*, 1998, **5**, 297.
6 B. Akdim, R. Pachter, X. Duan and W. W. Adams, *Phys. Rev. B*, 2003, **67**, 245404.
7 P. Bracke, H. Schurmans and J. Verhoest, *Inorganic Fibres and Composite Materials: A Survey of Recent Developments*, Pergamon, New York, 1984.
8 X. Blase, J. C. Charlier, A. De Vita and R. Car, *Appl. Phys. A*, 1999, **68**, 293.
9 M. O. Watanabe, S. Itoh, T. Sasaki and K. Mizushima, *Phys. Rev. Lett.*, 1996, **77**, 187.
10 J. B. Yoo, J. H. Han, S. H. Choi, T. Y. Lee, C. Y. Park, T. W. Jeong, J. H. Lee, S. Yu, G. Park, W. K. Yi, H. S. Kim, Y.-J. Baik and J. M. Kim, *Physica B*, 2002, **323**, 180.
11 P. Dorozhkin, D. Goldberg, Y. Bando and Z.-C. Dong, *Appl. Phys. Lett.*, 2002, **81**, 1083.
12 R. Ma, Y. Bando, H. Zhu, T. Sato, C. Xu and D. Wu, *J. Am. Chem. Soc.*, 2002, **124**, 7672.
13 C. Tang, Y. Bando, X. Ding, S. Qi and D. Goldberg, *J. Am. Chem. Soc.*, 2002, **124**, 14550.
14 L. J. Terminello, A. Chaiken, D. A. Lapiano-Smith, G. L. Doll and T. Sato, *J. Vac. Sci. Technol. A*, 1994, **12**, 2462.
15 I. Jimenez, A. Jankowski, L. J. Terminello, J. A. Carlisle, D. G. J. Sutherland, G. L. Doll, J. V. Mantese, W. M. Tong, D. K. Shuh and F. J. Himpsel, *Appl. Phys. Lett.*, 1996, **68**, 2816.
16 J. Ager III, D. Veirs and G. Rosenblatt, *Phys. Rev. B*, 1991, **43**, 6491.
17 D. M. Gruen, A. R. Krauss, C. D. Zuiker, R. Csencsits, L. J. Terminello, J. A. Carlisle, I. Jimenez, D. G. J. Sutherland, D. K. Shuh, W. Tong and F. J. Himpsel, *Appl. Phys. Lett.*, 1996, **68**, 1640.
18 J. Stöhr, *NEXAFS Spectroscopy*, Springer-Verlag, Berlin, 1992.
19 J. Moscovici, G. Loupias, P. Parents and G. Tourillon, *J. Phys. Chem. Solids*, 1996, **57**, 1159.
20 A. Chaiken, L. J. Terminello, J. Wong, G. L. Doll and C. A. Taylor, *Appl. Phys. Lett.*, 1993, **63**, 2112.
21 I. Jimenez, A. F. Jankowski, L. J. Terminello, D. G. J. Sutherland, J. A. Carlisle, G. L. Doll, W. M. Tong, D. K. Shuh and F. J. Himpsel, *Phys. Rev. B*, 1997, **55**, 12025.
22 I. Shimoyama, Y. Baba, T. Sekiguchi and K. G. Nath, *J. Electron. Spectrosc. Relat. Phenom.*, 2004, **137–140**, 573.
23 D. H. Berns, M. A. Cappelli and D. K. Shuh, *Diamond Relat. Mater.*, 1997, **6**, 1883.
24 S. Banerjee, T. Hemraj-Benny, M. Balasubramanian, D. A. Fischer, J. A. Misewich and S. S. Wong, *Chem. Commun.*, 2004, 772.
25 S. Banerjee, T. Hemraj-Benny, M. Balasubramanian, D. A. Fischer, J. A. Misewich and S. S. Wong, *ChemPhysChem*, 2004, **5**, 1416.
26 M. Terrones, N. Grobert and H. Terrones, *Carbon*, 2002, **40**, 1665.
27 W. Han, Y. Bando, K. Kurashima and T. Sato, *Appl. Phys. Lett.*, 1998, **73**, 3085.
28 D. Golberg, W. Han, Y. Bando, L. Bourgeois, K. Kurashima and T. Sato, *J. Appl. Phys.*, 1999, **86**, 2364.
29 D. Golberg, Y. Bando, W. Han, K. Kurashima and T. Sato, *Chem. Phys. Lett.*, 1999, **308**, 337.
30 A. S. Vinogradov, S. V. Nekipelov and A. A. Pavlychev, *Sov. Phys. Solid State*, 1991, **33**, 508.
31 Z. Fu, personal communication.
32 I. Tanaka, H. Araki, M. Yoshiya, T. Mizoguchi, K. Ogasawara and H. Adachi, *Phys. Rev. B*, 1999, **60**, 4944.
33 A. Loiseau, F. Williame, N. Demoncy, N. Schramchenko, G. Hug, C. Colliex and H. Pascard, *Carbon*, 1998, **36**, 743.
34 W. H. Moon and H. J. Hwang, *Physica E*, 2004, **23**, 26.
35 M. Terauchi, M. Tanaka, T. Matsumoto and Y. Saito, *J. Electron Microsc.*, 1998, **47**, 319.
36 S. E. Rodil and S. Muhl, *Diamond Rel. Mater.*, 2004, **13**, 1521.
37 N. Mubumbila, B. Bouchet-Fabre, C. Godon, C. Marhic, B. Angleraud, P.-Y. Tessier and T. Minea, *Diamond Rel. Mater.*, 2004, **13**, 1433.

